Laser stimulated thermal conductivity in chiral carbon nanotube

A. Twum[1], S. Y. Mensah[1], N. G. Mensah[2], K. A. Dompreh[1], S. S. Abukari[1] and M. Rabiu[3]

[1] Department of Physics, Laser and Fiber Optics Center, University of Cape Coast, Cape Coast, Ghana.
[2] Department of Mathematics, University of Cape Coast, Cape Coast, Ghana.
[3] Department of Applied Physics, Faculty of Applied Sciences, University for Development Studies, Navrongo Campus, Ghana.

E-mail: `+233 042 33837, profsymensah@yahoo.co.uk`

Abstract. An investigation of laser stimulated thermal conductivity in chiral CNT is presented. The thermal conductivity of a chiral CNT is calculated using a tractable analytical approach. This is done by solving the Boltzmann transport equation with energy dispersion relation obtained in the tight binding approximation. The electron thermal conductivity along the circumferential χ_c and axial χ_z are obtained. The results obtained are numerically analyzed and both χ_c and χ_z are found to oscillate in the presence of laser radiations. We have also noted that the laser source caused a drastic reduction in the both χ_c and χ_z values.

1. Introduction

Carbon-based materials (diamond and in-plane graphite) display the highest measured thermal conductivity of any known material at moderate temperatures [1]. The discovery of carbon nanotubes in 1991 [2] has led to speculation that this new material could have a thermal conductivity greater than that of diamond and graphite [3]. Carbon nanotube has found a lot of application in electronic and mechanical devices. It is, therefore, not surprising that the material has received a lot of attention over the past decade [4-11].

The thermal conductivity of materials in general is partitioned into charge carriers (i.e., electron or hole) component χ_e which depends on the electronic band structure, electron scattering and electron-phonon interaction, and lattice component χ_L which depends mainly on phonon and phonon scattering. In dielectrics, $\chi_L \gg \chi_e$ while in metals the reverse is the case. In semiconductors, the value of the thermal conductivity χ is strongly dependent on the composition of the semiconductor, and the value of χ_L is generally greater than the value of χ_e.

So far, most publications on the thermal conductivity of carbon nanotubes have paid attention to only the lattice thermal conductivity and completely neglected electron thermal conductivity. Hone et al. [3] found that the conductivity of carbon nanotubes was temperature dependent, and was almost a linear relationship. They suggested that the conductivity decreases smoothly with temperature, and displays linear temperature dependence below 30 K. However, Berber et al. [12] suggested that the graph of the temperature dependence of thermal conductivity looked less linear and that it shows a positive slope from low temperatures up to 100 K where it peaks around 37000 W/mK. Then, the thermal conductivity drops dramatically down to around 3000 W/mK when the temperature approaches 400 K. Similar relationship has been found by Mensah et al. [13] for electron thermal conductivity χ_e.

Mensah et al. [14] have also studied the electron thermal conductivity of carbon nanotubes. They observed that the temperature dependence of χ_e in carbon nanotubes is similar to that obtained by Berber et al. and that χ_e peaks at unusually high values. They further observed the dependence of χ_e on the geometric chiral angle θ, temperature T, the real overlapping integrals for jumps along the tubular axis Δ_z and the base helix Δ_s. Interestingly, they again noted that varying these parameters could give rise to unusual high electron thermal conductivity whose peak values shift towards higher temperatures. For example, at $\Delta_z = 0.02$ eV and $\Delta_s = 0.015$ eV. The peak value of χ_e occurs at 104K and is about 41000 W/mK which compares well with that reported for a 99.9% isotropically enriched 12C diamond crystal. In this work, we will use the approach in [15] to investigate theoretically the laser stimulated thermal conductivity in chiral CNTs. In this paper we consider the effect of laser on the thermal conductivity of chiral carbon nanotube. We observed that the laser has drastic effect on the electron thermal conductivity. It drastically reduced the thermal conductivity i.e. about 10 times. It also causes χ to oscillate with the amplitude of the laser source.

The paper is organized as follows: section one deal with the introduction; in section two, we establish the theory and solutions; results obtained will be discussed in section three and finally we draw our conclusions

2. Theory

The thermal current density q and electron thermal conductivity χ of a chiral SWNT are calculated as functions of the geometric chiral angle θ_h, temperature T, the real overlapping integrals for jumps along the nanotube axis Δ_z and along the base helix Δ_s. The calculation is done using the approach in reference [15] together with the phenomenological model of a SWNT developed in references [16] and [17]. This model yields physically interpretable results and gives correct qualitative descriptions of various electronic processes, which are corroborated by the first-principle numerical simulations of Miyamoto *et. al.* [18].

Following the approach of [19], we consider a SWNT under a temperature gradient ∇T and placed in an electric field applied along the nanotube axis. Employing the Boltzmann kinetic equation

$$\frac{\partial f(r,p,t)}{\partial t} + v(p)\frac{\partial f(r,p,t)}{\partial r} + eE(t)\frac{\partial f(r,p,t}{\partial p} = \frac{\partial(r,p,t) - f_0(p)}{\tau} \qquad (1)$$

where $f(r,p,t)$ is the distribution function, $f_0(p)$ is the equilibrium distribution function, $v(p)$ is the electron velocity, $E(t) = E_0 + E_1 cos(\omega t)$ is the magnitude of the electric field, with E_0 being constant electric field and $E_1 cos(\omega t)$ being monochromatic laser source, r is the electron position, p is the electron dynamical momentum, t is time elapsed, τ is the electron relaxation time and e is the electron charge and taken the collision integral in the τ approximation and further assumed constant, the exact solution of (1) is solved using perturbation approach where the second term is treated as the perturbation. In the linear approximation of ∇T and $\nabla \mu$, the solution to the Boltzmann kinetic equation is

$$f(p,t) = \tau^{-1} \int_0^\infty \exp\left(-\frac{t}{\tau}\right) f_0\left(p - e\int_{t-t'}^t \left[E_0 + E_1 \cos \omega t''\right] dt''\right) dt + \cdots$$

$$\int_0^\infty \exp\left(-\frac{t}{\tau}\right) dt \left\{\left[\varepsilon\left(p - e\int_{t-t'}^t \left[E_0 + E_1 \cos wt''\right] dt''\right) - \mu\right]\frac{\nabla T}{T} + \nabla\mu\right\}$$

$$\times v\left(p - e\int_{t-t'}^t \left[E_0 + E_1 \cos \omega t''\right] dt''\right)$$

$$\times \frac{\partial f_0}{\partial \varepsilon}\left(p - e\int_{t-t'}^t \left[E_0 + E_1 \cos wt''\right] dt''\right) \qquad (2)$$

$\varepsilon(p)$ is the tight-binding energy of the electron, and μ is the chemical potential. The thermal current density q is defined as

$$q = \sum_p \left[\varepsilon(p) - \mu\right] v(p) f(p). \qquad (3)$$

Substituting (2) into (3) we have

$$q = \tau^{-1} \int_0^\infty \exp(-\frac{t}{\tau})dt \sum_p [\varepsilon(p) - \mu]v(p)f_0\left(p - e\int_{t-t'}^t [E_0 + E_1 \cos \omega t''] dt''\right)$$

$$+ \int_0^\infty \exp\left(-\frac{t}{\tau}\right) dt \sum_p [\varepsilon(p) - \mu] v(p)$$

$$\times \left\{ \left[\varepsilon\left(p - e\int_{t-t'}^t [E_0 + E_1 \cos \omega t''] dt'' - \mu\right)\right] \frac{\nabla T}{T} + \nabla \mu \right\}$$

$$\times v\left(p - e\int_{t-t'}^t [E_0 + E_1 \cos \omega t''] dt''\right) \frac{\partial f_0}{\partial \varepsilon}\left(p - e\int_{t-t'}^t [E_0 + E_1 \cos \omega t''] dt''\right) \quad (4)$$

Making the transformation

$$p - e\int [E_0 + E_1 \cos wt''] dt'' \to p,$$

we obtain for the thermal current density

$$q = \tau^{-1} \int_0^\infty \exp\left(-\frac{t}{\tau}\right) dt \sum_p \left[\varepsilon\left(p - e\int_{t-t'}^t [E_0 + E_1 \cos wt''] dt''\right) - \mu\right]$$

$$\times v\left(p - e\int_{t-t'}^t [E_0 + E_1 \cos wt''] dt''\right) f_0(p) \dots$$

$$+ \int_0^\infty \exp\left(-\frac{t}{\tau}\right) dt \sum_p \left[\varepsilon\left(p - e\int_{t-t'}^t [E_0 + E_1 \cos \omega t''] dt''\right) - \mu\right]$$

$$\times \left\{[\varepsilon(p) - \mu]\frac{\nabla T}{T} + \nabla \mu\right\} \left\{v(p)\frac{\partial f_0(p)}{\partial \varepsilon}\right\}$$

$$\times v\left(p - e\int_{t-t'}^t [E_0 + E_1 \cos \omega t''] dt''\right) \quad (5)$$

Using the phenomenological model in [16, 17, 20], a SWNT is considered as an infinitely long periodic chain of carbon atoms wrapped along a base helix and the thermal current density is written in the form

$$q = S'u_s + Z'u_z \quad (6)$$

where S' and Z' are respectively components of the thermal current density along the base helix and along the nanotube axis. The motion of electrons in the SWNT is resolved along the nanotube axis in the direction of the unit vector u_z and a unit vector u_s tangential to the base helix. u_c is defined as the unit vector tangential to the circumference of the nanotube and θ_h is the geometric chiral angle (GCA). u_c is always perpendicular to u_z, therefore u_s can be resolved along u_c and u_z as

$$u_s = u_c cos\theta_h + u_z sin\theta_h. \quad (7)$$

Therefore, j can be expressed in terms of u_c and u_z as

$$q = u_c(S'cos\theta_h) + u_z(Z' + S'sin\theta_h) \equiv j_c u_c + j_z u_z \quad (8)$$

which implies that,

$$q_c = S' \cos\theta_h \tag{9}$$

$$q_z = Z' + S' \sin\theta_h \tag{10}$$

The interference between the axial and helical paths connecting a pair of atoms is neglected so that transverse motion quantization is ignored [16, 17]. This approximation best describes doped chiral carbon nanotubes, and is experimentally confirmed in [21]. Thus if in (5) the transformation

$$\sum_p \to \frac{2}{(2\pi\hbar)^2} \int_{-\frac{\pi}{d_s}}^{\frac{\pi}{d_s}} dP_s \int_{-\frac{\pi}{d_z}}^{\frac{\pi}{d_z}} dP_z$$

is made, Z and S respectively become,

$$Z' = \frac{2}{(2\pi\hbar)^2} \int_0^\infty \exp\left(-\frac{t}{\tau}\right) dt \int_{-\frac{\pi}{d_s}}^{\frac{\pi}{d_s}} dP_s \int_{-\frac{\pi}{d_z}}^{\frac{\pi}{d_z}} dP_z \left[\varepsilon\left(p - e\int_{t-t'}^t [E_0 + E_z \cos\omega t''] dt''\right) - \mu\right]$$

$$\times v_z\left(p - e\int_{t-t'}^t [E_0 + E_s \cos wt''] dt''\right) \left[\tau^{-1} f_0(p) + \cdots\right.$$

$$\left.\left\{[\varepsilon(p) - \mu]\frac{\nabla_z T}{T} + \nabla_z \mu\right\}\left\{v_z(p)\frac{\partial f_0(p)}{\partial \varepsilon}\right\}\right] \tag{11}$$

and

$$S' = \frac{2}{(2\pi\hbar)^2} \int_0^\infty \exp\left(-\frac{t}{\tau}\right) dt \int_{-\frac{\pi}{d_s}}^{\frac{\pi}{d_s}} dP_s \int_{-\frac{\pi}{d_z}}^{\frac{\pi}{d_z}} dP_z \left[\varepsilon\left(p - e\int_{t-t'}^t [E_0 + E_s \cos\omega t''] dt''\right) - \mu\right]$$

$$\times v_s\left(p - e\int_{t-t'}^t [E_0 + E_z \cos wt''] dt''\right) \left[\tau^{-1} f_0(p) + \cdots\right.$$

$$\left.\left\{[\varepsilon(p) - \mu]\frac{\nabla_s T}{T} + \nabla_s \mu\right\}\left\{v_s(p)\frac{\partial f_0(p)}{\partial \varepsilon}\right\}\right] \tag{12}$$

where the integrations are carried out over the first Brillouin zone, $\hbar$ is Planck's constant, v_s, p_s, E_s, $\nabla_s T$, and $\nabla_s \mu$ are the respective components of v, p, E, ∇T and $\nabla \mu$ along the base helix, and v_z, p_z, E_z, $\nabla_z T$, and $\nabla_z \mu$ are the respective components along the nanotube axis.

The energy dispersion relation for a chiral nanotube obtained in the tight binding approximation [16] is

$$\varepsilon(p) = \varepsilon_0 - \Delta_s \cos\frac{P_s d_s}{\hbar} - \Delta_z \cos\frac{P_z d_z}{\hbar} \tag{13}$$

where ε_0 is the energy of an outer-shell electron in an isolated carbon atom, Δ_z and Δ_s are the real overlapping integrals for jumps along the respective coordinates, p_s and p_z are the components of momentum tangential to the base helix and along the the nanotube axis, respectively. The components v_s and v_z of the electron velocity V are respectively calculated from the energy dispersion relation 13 as

$$v_s(p) = \frac{\partial \varepsilon(p)}{\partial P_s} = \frac{\Delta_s d_s}{\hbar} \sin\frac{P_s d_s}{\hbar} \tag{14}$$

$$v_s\left(p - e\int_{t-t'}^{t}\left[E_0 + E_1\cos wt''\right]dt''\right) = \frac{\Delta_s d_s}{\hbar}\sin\left(p - e\int_{t-t'}^{t}\left[E_0 + E_1\cos wt''\right]dt''\right)$$

$$= \frac{\Delta_s d_s}{\hbar}\left\{\sin\frac{P_s d_s}{\hbar}\cos\left(p - e\int_{t-t'}^{t}\left[E_0 + E_1\cos wt''\right]dt''\right)\right\}$$

$$-\cos\frac{P_s d_s}{\hbar}\sin\left(p - e\int_{t-t'}^{t}\left[E_0 + E_1\cos wt''\right]dt''\right). \tag{15}$$

Also,

$$v_z(p) = \frac{\partial\varepsilon(p)}{\partial P_z} = \frac{\Delta_z d_z}{\hbar}\sin\frac{P_z d_z}{\hbar}, \tag{16}$$

and

$$v_z\left(p - e\int_{t-t'}^{t}\left[E_0 + E_1\cos wt''\right]dt''\right) =$$

$$\frac{\Delta_z d_z}{\hbar}\left\{\sin\frac{P_s d_s}{\hbar}\cos\left(p - e\int_{t-t'}^{t}\left[E_0 + E_1\cos wt''\right]dt''\right)\right\}$$

$$-\cos\frac{P_z d_z}{\hbar}\sin\left(p - e\int_{t-t'}^{t}\left[E_0 + E_1\cos wt''\right]dt''\right). \tag{17}$$

To calculate the carrier current density for a non-degenerate electron gas, the Boltzmann equilibrium distribution function $f_0(p)$ is expressed as

$$f_0(p) = C\exp\left(\frac{\Delta_s\cos\frac{P_s d_s}{\hbar} + \Delta_z\cos\frac{P_z d_z}{\hbar} + \mu - \varepsilon_0}{kT}\right). \tag{18}$$

Where C is found to be

$$C = \frac{d_s d_z n_0}{2I_0(\Delta_s^*)I_0(\Delta_z^*)}\exp\left(-\frac{\mu - \varepsilon_0}{kT}\right) \tag{19}$$

and n_0 is the surface charge density, $I_n(x)$ is the modified Bessel function of order n defined by $\Delta_s^* = \frac{\Delta_s}{kT}$ and $\Delta_z^* = \frac{\Delta_z}{kT}$ and k is Boltzmann's constant.

Now, we substituted Eqs.(13) and (18) into Eqs.(11) and (12), and carried out the integrals. After cumbersome calculations the following expressions were obtain

$$S' = -\sigma_s(E)\frac{1}{e}\left\{(\varepsilon_0 - \mu)\sum_{n=-\infty}^{\infty}J_n^2(a) - \frac{\Delta_s}{2}\left(1 + 3\sum_{n=-\infty}^{\infty}J_n^2(a)\right)\left(\frac{I_0(\Delta_z^*)}{I_1(\Delta_z^*)} - \frac{2}{\Delta_s^*}\right)\right.$$

$$\left.-\Delta_s\frac{I_1(\Delta_z^*)}{I_0(\Delta_z^*)}\sum_{n=-\infty}^{\infty}J_n^2(a)\right\}E_{sn}^*$$

$$-\sigma_s(E)\frac{k}{e^2}\left\{\frac{(\varepsilon_0 - \mu)^2}{kT}\sum_{n=-\infty}^{\infty}J_n^2(a) - \frac{\Delta_s}{2}\frac{(\varepsilon_0 - \mu)}{kT}\left(1 + 3\sum_{n=-\infty}^{\infty}J_n^2(a)\right)\right.$$

$$\times\left(\frac{I_0(\Delta_z^*)}{I_1(\Delta_z^*)} - \frac{2}{\Delta_s^*}\right) - 2\Delta_s\frac{(\varepsilon_0 - \mu)}{kT}\frac{I_1(\Delta_z^*)}{I_0(\Delta_z^*)}\sum_{n=-\infty}^{\infty}J_n^2(a)$$

$$\left.+\frac{\Delta_s\Delta_s^*}{2}\left(1 - \frac{3I_0(\Delta_s^*)}{I_1(\Delta_s^*)} + \frac{6}{\Delta_s^{*2}}\right)\left(1 + \sum_{n=-\infty}^{\infty}J_n^2(a)\right)\right.$$

$$+\frac{\Delta_s \Delta_s^*}{2}\left(\frac{I_0(\Delta_s^*)}{I_1(\Delta_s^*)}-\frac{2}{\Delta_s^*}\right)\left(1+3\sum_{n=-\infty}^{\infty}J_n^2(a)\right)$$

$$+\Delta_z\Delta_z^*\left(1-\frac{I_1(\Delta_z^*)}{\Delta_z^*I_0(\Delta_z^*)}\right)\sum_{n=-\infty}^{\infty}J_n^2(a)\bigg\}\nabla_sT \tag{20}$$

$$Z'=-\sigma_z(E)\frac{1}{e}\bigg\{(\varepsilon_0-\mu)\sum_{n=-\infty}^{\infty}J_n^2(a)-\frac{\Delta_z}{2}\left(1+3\sum_{n=-\infty}^{\infty}J_n^2(a)\right)\left(\frac{I_0(\Delta_z^*)}{I_1(\Delta_z^*)}-\frac{2}{\Delta_s^*}\right)$$

$$-\Delta_s\frac{I_1(\Delta_s^*)}{I_0(\Delta_s^*)}\sum_{n=-\infty}^{\infty}J_n^2(a)\bigg\}E_{zn}^*$$

$$-\sigma_z(E)\frac{k}{e^2}\bigg\{\frac{(\varepsilon_0-\mu)^2}{kT}\sum_{n=-\infty}^{\infty}J_n^2(a)-\frac{\Delta_z}{2}\frac{(\varepsilon_0-\mu)}{kT}\left(1+3\sum_{n=-\infty}^{\infty}J_n^2(a)\right)$$

$$\times\left(\frac{I_0(\Delta_s^*)}{I_1(\Delta_s^*)}-\frac{2}{\Delta_z^*}\right)-2\Delta_s\frac{(\varepsilon_0-\mu)}{kT}\frac{I_1(\Delta_z^*)}{I_0(\Delta_z^*)}\sum_{n=-\infty}^{\infty}J_n^2(a)$$

$$+\frac{\Delta_z\Delta_z^*}{2}\left(1-\frac{3I_0(\Delta_z^*)}{I_1(\Delta_z^*)}+\frac{6}{\Delta_{z^2}^*}\right)\left(1+\sum_{n=-\infty}^{\infty}J_n^2(a)\right)$$

$$+\frac{\Delta_z\Delta_s^*}{2}\left(\frac{I_0(\Delta_z^*)}{I_1(\Delta_z^*)}-\frac{2}{\Delta_z^*}\right)\left(1+3\sum_{n=-\infty}^{\infty}J_n^2(a)\right)$$

$$+\Delta_s\Delta_s^*\left(1-\frac{I_1(\Delta_s^*)}{\Delta_s^*I_0(\Delta_s^*)}\right)\sum_{n=-\infty}^{\infty}J_n^2(a)\bigg\}\nabla_zT \tag{21}$$

Where we have defined E_{sn}^* as

$$E_{sn}^*=E_n+\nabla_s\frac{\mu}{e},$$

and $\sigma_i(E)$ as

$$\sigma_s(E)=\frac{e^2\tau\Delta_s d_s^2 n_0}{\hbar^2}\frac{I_1(\Delta_s^*)}{I_0(\Delta_s^*)}, \qquad i=s,\,z \tag{22}$$

with $J_n(a)$ in Eqs.20 and 21 is the bessel function of the nth order. $a=ed_sE_s/\omega\hbar$. E_i is the amplitude of the laser. Substituting Eq.20 into Eq.9 gives circumferential thermal current density q_c as

$$q_c=-\sigma_s(E)\frac{kT}{e}\sin\theta_h\cos\theta_h$$

$$\times\bigg\{\xi\sum_{n=-\infty}^{\infty}J_n^2(a)-\frac{\Delta_s^*}{2}B_s\left(1+3\sum_{n=-\infty}^{\infty}J_n^2(a)\right)-\Delta_z^*A_z\sum_{n=-\infty}^{\infty}J_n^2(a)\bigg\}E_{zn}^*$$

$$-\sigma_s(E)\frac{k^2T}{e^2}\sin\theta_h\cos\theta_h\bigg\{\xi^2\sum_{n=-\infty}^{\infty}J_n^2(a)-\frac{\Delta_s^*}{2}\xi B_s\left(1+3\sum_{n=-\infty}^{\infty}J_n^2(a)\right)$$

$$-2\Delta_z^*\xi A_z\sum_{n=-\infty}^{\infty}j_n^2(a)+\frac{(\Delta_s^*)^2}{2}C_s\left(1+\sum_{n=-\infty}^{\infty}j_n^2(a)\right)+\frac{\Delta_s^*\Delta_z^*}{2}B_sA_z$$

$$\times \left(1 + 3 \sum_{n=-\infty}^{\infty} j_n^2(a)\right) + (\Delta_s^*)^2 \left(1 - \frac{A_z}{\Delta_z}\right) \sum_{n=-\infty}^{\infty} j_n^2(a)\right\} \Delta_z T. \tag{23}$$

Also, substituting Eq.(21) into Eq.(10) gives axial thermal current density qz as

$$q_z = -\frac{kT}{e} \left\{ \sigma_z(E) \left[\xi \sum_{n=-\infty}^{\infty} J_n^2(a) - \frac{\Delta_z^*}{2} B_z \left(1 + 3 \sum_{n=-\infty}^{\infty} J_n^2(a)\right) - \Delta_s^* A_s \sum_{n=-\infty}^{\infty} J_n^2(a) \right] \right.$$

$$+ \sigma_s(E) \sin^2 \theta_h \left[\xi \sum_{n=-\infty}^{\infty} J_n^2(a) - \frac{\Delta_s^*}{2} B_s \left(1 + 3 \sum_{n=-\infty}^{\infty} J_n^2(a)\right) \right.$$

$$\left.\left. - \Delta_z^* A_z \sum_{n=-\infty}^{\infty} J_n^2(a) \right] \right\} E_{zn}^*$$

$$- \frac{k^2 T}{e^2} \left\{ \sigma_z(E) \left[\xi^2 \sum_{n=-\infty}^{\infty} J_n^2(a) - \frac{\Delta_z^*}{2} \xi B_z \left(1 + 3 \sum_{n=-\infty}^{\infty} J_n^2(a)\right) \right. \right.$$

$$- 2\Delta_s^* \xi A_s \sum_{n=-\infty}^{\infty} J_n^2(a) + \frac{(\Delta_z^*)^2}{2} C_z \left(1 + \sum_{n=-\infty}^{\infty} J_n^2(a)\right)$$

$$\left. + \frac{\Delta_z^* \Delta_s^*}{2} A_s B_z \left(1 + 3 \sum_{n=-\infty}^{\infty} J_n^2(a)\right) + (\Delta_s^*)^2 \left(1 - \frac{A_s}{\Delta_s^*}\right) \sum_{n=-\infty}^{\infty} J_n^2(a) \right]$$

$$+ \sigma_s(E) \sin^2 \theta_h \left[\xi^2 \sum_{n=-\infty}^{\infty} J_n^2(a) - \frac{\Delta_s^*}{2} \xi B_s \left(1 + 3 \sum_{n=-\infty}^{\infty} J_n^2(a)\right) \right.$$

$$- 2\Delta_z^* \xi A_z \sum_{n=-\infty}^{\infty} J_n^2(a) + \frac{(\Delta_s^*)^2}{2} C_s \left(1 + \sum_{n=-\infty}^{\infty} J_n^2(a)\right) + \frac{\Delta_s^* \Delta_z^*}{2} A_z B_s$$

$$\left.\left. \times \left(1 + 3 \sum_{n=-\infty}^{\infty} J_n^2(a)\right) + (\Delta_z^*)^2 \left(1 - \frac{A_z}{\Delta_z^*}\right) \sum_{n=-\infty}^{\infty} J_n^2(a) \right] \right\} \nabla_z T. \tag{24}$$

Here we have used the following definitions

$$\xi = \frac{\varepsilon_0 - \mu}{kT}, \quad A_i = \frac{I_1(\Delta_i^*)}{I_0(\Delta_i^*)}, \quad B_i = \frac{I_0(\Delta_i^*)}{I_1(\Delta_i^*)} - \frac{2}{\Delta_i^*}, \quad C_i = 1 - \frac{3 I_0(\Delta_i^*)}{\Delta_i^* I_1(\Delta_i^*)} + \frac{6}{\Delta_i^{*2}}. \tag{25}$$

The circumferential χ_{ec} and axial χ_{ez} components of the electron thermal conductivity in the CNT are obtained from Eqs (23) and (24) respectively. In fact the coefficients of the temperature gradient in these equations define χ_{ec} and χ_{ez} as follows,

$$\chi_{ec} = \sigma_s(E) \frac{k^2 T}{e^2} \sin \theta_h \cos \theta_h \left\{ \xi^2 \sum_{n=-\infty}^{\infty} J_n^2(a) - \frac{\Delta_s^*}{2} \xi B_s \left(1 + 3 \sum_{n=-\infty}^{\infty} J_n^2(a)\right) \right.$$

$$- 2\Delta_z^* \xi A_z \sum_{n=-\infty}^{\infty} J_n^2(a) + \frac{(\Delta_s^*)^2}{2} C_s \left(1 + \sum_{n=-\infty}^{\infty} J_n^2(a)\right)$$

$$\left. + \frac{\Delta_s^* \Delta_z^*}{2} B_s A_z \left(1 + 3 \sum_{n=-\infty}^{\infty} J_n^2(a)\right) + (\Delta_z^*)^2 \left(1 - \frac{A_z}{\Delta_z^*}\right) \sum_{n=-\infty}^{\infty} J_n^2(a) \right\} \tag{26}$$

$$\chi_{ez} = \frac{k^2 T}{e^2} \left\{ \sigma_z(E) \left[\xi^2 \sum_{n=-\infty}^{\infty} J_n^2(a) - \frac{\Delta_z^*}{2} \xi B_z \left(1 + 3 \sum_{n=-\infty}^{\infty} J_n^2(a) \right) - 2\Delta_s^* \xi A_s \sum_{n=-\infty}^{\infty} J_n^2(a) \right. \right.$$

$$+ \frac{(\Delta_z^*)^2}{2} C_z \left(1 + \sum_{n=-\infty}^{\infty} J_n^2(a) \right) + \frac{\Delta_z^* \Delta_s^*}{2} A_s B_z \left(1 + 3 \sum_{n=-\infty}^{\infty} J_n^2(a) \right)$$

$$\left. + (\Delta_s^*)^2 \left(1 - \frac{A_s}{\Delta_s^*} \right) \sum_{n=-\infty}^{\infty} J_n^2(a) \right] + \sigma_s(E) \sin^2\theta_h \left[\xi^2 \sum_{n=-\infty}^{\infty} J_n^2(a) \right.$$

$$- \frac{\Delta_s^*}{2} \xi B_s \left(1 + 3 \sum_{n=-\infty}^{\infty} J_n^2(a) \right) - 2\Delta_z^* \xi A_z \sum_{n=-\infty}^{\infty} J_n^2(a)$$

$$+ \frac{(\Delta_s^*)^2}{2} C_s \left(1 + \sum_{n=-\infty}^{\infty} J_n^2(a) \right) + \frac{\Delta_s^* \Delta_z^*}{2} A_z B_s \left(1 + 3 \sum_{n=-\infty}^{\infty} J_n^2(a) \right)$$

$$\left. \left. + (\Delta_z^*)^2 \left(1 - \frac{A_z}{\Delta_z^*} \right) \sum_{n=-\infty}^{\infty} J_n^2(a) \right] \right\}. \tag{27}$$

In summary, the analytical expressions obtained for the thermal current density q and electron thermal conductivity χ depend on the geometric chiral angle θ_h, temperature T, the real overlapping integrals for jumps along the tubular axis Δ_z and the base helix Δ_s.

When the Laser source is switched off i.e. $E_s = 0$, the circumferential and axial components of the electron thermal conductivity expressions in Eqs.(**??**) and (27) reduces to

$$\chi_{ec} = \sigma_s(E) \frac{k^2 T}{e^2} \sin\theta_h \cos\theta_h \left\{ \xi^2 - 2\Delta_s^* \xi B_s - 2\Delta_z^* \xi A_z + (\Delta_s^*)^2 C_s \right.$$

$$\left. + 2\Delta_s^* \Delta_z^* B_s A_z + (\Delta_z^*)^2 \left(1 - \frac{A_z}{\Delta_z^*} \right). \tag{28}$$

$$\chi_{ez} = \frac{k^2 T}{e^2} \left\{ \sigma_z(E) \left[\xi^2 - 2\Delta_z^* \xi B_z - 2\Delta_s^* \xi A_s + 2(\Delta_z^*)^2 C_z + 2\Delta_z^* \Delta_s^* A_s B_z \right. \right.$$

$$\left. + (\Delta_s^*)^2 \left(1 - \frac{A_s}{\Delta_s^*} \right) \right] + \sigma_s(E) \sin^2\theta_h \left[\xi^2 - 2\Delta_s^* \xi B_s - 2\Delta_z^* \xi A_z \right.$$

$$\left. \left. + 2(\Delta_s^*)^2 C_s + 2\Delta_s^* \Delta_z^* A_z B_s + (\Delta_z^*)^2 \left(1 - \frac{A_z}{\Delta_z^*} \right) \right] \right\}. \tag{29}$$

which are obtained in [13].

3. Results, Discussion and Conclusion

The Boltzmann transport equation was utilized to obtain expressions of the thermal current density and electron thermal conductivity of chiral SWNT.

We observed from (**??**) and (27) that the electron thermal conductivity of a chiral CNT is dependent on the electric field E_s, temperature T, GCA θ_h, and the overlapping integrals Δ_s and Δ_z for jumps along the circumferential and axial directions. Using MATLAB we sketched (**??**) and (27) to show how these parameters affect the electron thermal conductivity of a chiral CNT.

Figure (1a) represents the dependence of circumferential electron thermal conductivity, χ_c, on temperature for a fixed value of $\Delta_s = 0.010$eV and values of Δ_z varied from 0.010eV to 0.014eV. We noticed that the relationship between χ_c and T is nonlinear and indicates a positive slope at low temperatures and negative slope at high temperatures. The physical interpretation to the part of the graph showing positive slope is that more electrons are thermally generated to transport heat through the chiral CNT. The peak of the graph indicates the threshold temperature at which electron and heat transport through the chiral CNT is maximum. The negative slope of the graph shows that as temperature exceeds the threshold value, carbon atoms are energized to vibrate faster thereby scattering the electrons carrying thermal energies through the chiral CNT. At temperatures above 300K, χ_c assumes a lower constant value for all values of Δ_z. The peak values of χ_c were found to decrease as Δ_z increases. Figure (1b) shows the dependence of χ_c, on temperature for GCA θ_h varied between 1.2^o and 2.0^o. It was noted that the values of χ_c increases with increasing GCA θ_h.

Figure (1c) represents the dependence of axial electron thermal conductivity, χ_z, on temperature T for a fixed value of $\Delta_s = 0.010$eV and values of Δ_z varied from 0.010eV to 0.015eV. Like χ_c, the relationship between χ_z and T is also found to be nonlinear and indicates a positive slope at low temperatures and negative slope at high temperatures. It was observed that as Δ_z increases, the values of χ_z also increase. It is quite interesting to note that the values of χ_z are much larger as compared with those of χ_c.

Electron thermal conductivities χ_c and χ_z dependence on temperature in the presence and also absence of Laser is sketched and presented as Figures (2a) and (2b). In comparison, we noted that the presence of laser causes a drastic reduction in χ_c and χ_z. The reason is that the Laser source E_s energizes the carbon atoms within the walls of the CNT and set them vibrating at large amplitudes which tend to scatter the electrons carrying thermal energy.

Figures (3a) and (3b) illustrate the behaviour of χ_c and χ_z as the Laser source E_s is varied. We noticed that as the Laser source increases χ_c and χ_z drops off sharply and oscillates towards larger E_s values. As E_s values become larger, the amplitudes of oscillation decrease.

4. Conclusions

The electron thermal conductivity χ of chiral CNT induced with monochromatic laser have been investigated. The chiral CNT parameters Δ_s Δ_z, θ_h, and the laser source E_s were found to have influence on the electron thermal conductivity χ of chiral CNT.

Our results show that a greater percentage of the electron and heat transport is

along the axis of the chiral CNT. It was observed that an increase in Δ_z causes χ_c to decrease and χ_z to increase. Also an increase in θ_h made χ_c to rise but had no effect on χ_z. The parameters χ_c and χ_z were also found to be oscillating when the laser source E_s was varied. The results obtained indicated that the laser source caused a drastic reduction in the χ values. The reduced values recorded for χ_c and χ_z is a clear indication that the laser retains heat at the junctions of the chiral CNT which helps to maintain a large temperature gradient.

[1] Kaye G.W.C., and Laby T.H., Tables of Physical and Chemical Constant, sixteenth ed., *Longman*, London, 1995.

[2] Iijima S., *Nature* 56 354 (1991).

[3] Hone J., Whitney M., Piskoti C., and Zettl A *Phys, Rev.* B **59** 2514 (1999).

[4] Bonard J.M., Salvetat J.P, Stockli T.,and De Heer W.A., *Appl. Phys. Lett.* 73 918 (1998).

[5] Wang Q.H., Corrigan T.D., Dai T.Y., and Chang R.P.H., *Appl. Phys. Lett.* **70** 3308 (1997).

[6] De Heer W.A, Chatelain A.,and Ugarte D., *Science* **270** 1179 (1995)

[7] Rinzler A.G., Hafner J.H., Nikolaev P., Lou L., Kim S.G., Tomanekb D., Nordlander P., Colbert D.T., and Smalley R.E., *Science* **269** 1550. (1995)

[8] Semet V., Thien Binh Vu, Vincent P., Guillot D., Teo K.B.K, Chhowalla M., Amaratunga G.A.J., andMilne W.I., *Appl. Phys. Lett.* **81** 343 (2002)

[9] Dillon A.C., Jones K.M., Bekkedahl T.A, Kiag C.H., Bethune D.S., and Heben M.J., *Nature* **386** 377 (1997).

[10] Chico L., Crespi V.H., Benedict L.X. , Louie S.G., and Cohen M.L., *Phys. Rev. Lett.* **76** 971 (1996).

[11] Derycke V., Martel R., Appenzeller and J., Avouris Ph., *Nano Lett*, **9** 453 (2001).

[12] Berber S., Kwon Y.K., and Tomanek D., *Phys. Rev. Lett.* **84** 4613 (2000).

[13] Mensah S.Y, Allotey F.K.A, Nkrumah G.,and Mensah N.G., *Physical E* **23** 152 (2004).

[14] Mensah N. G., Nkrumah G., Mensah S. Y., Allotey F. K. A. Temperature Dependence of the Thermal Conductivity in Chiral Carbon Nanotubes, *Phys Lett A* **329** 369 (2004).

[15] S.Y.Mensah, A. Twum, N. G. Mensah, K. A. Dompreh, S. S. Abukari, G. Nkrumah-Buandoh, Effect of laser on thermopower of chiral carbon nanotube, Mesoscale and Nanoscale Physics (cond-mat.mes-hall) arXiv:1104.1913v1 (2011)

[16] Slepyan G. Ya., Maksimenko S. A., Lakhtakia A., Yevtushenko O. M., and Gusakov A. V., *Phys. Rev.* B **57** 16 9485 (1998).

[17] Yevtushenko O. M., Ya Slepyan G., Maksimenko S A, Lakhtakia A. and Romanov D. A., *Phys. Rev. Lett.* **79**, 1102 (1997)

[18] Miyamoto Y., Louie S. G. and Cohen M. L., *Phys. Rev. Lett*. **76** 2121 (1996).

[19] Mensah S.Y., Allotey F.K.A., Mensah N.G. and Nkrumah G., *J. Phys.* **13** 5653 (2001)

[20] Romanov D. A. and Kibis O. V, *Phys. Lett.* **A 178**, 335 (1993)

[21] Yi-Chun Su and Wen-Kuang Hsu, *Appl. Phys. Lett.* **87**, 233112 (2005)
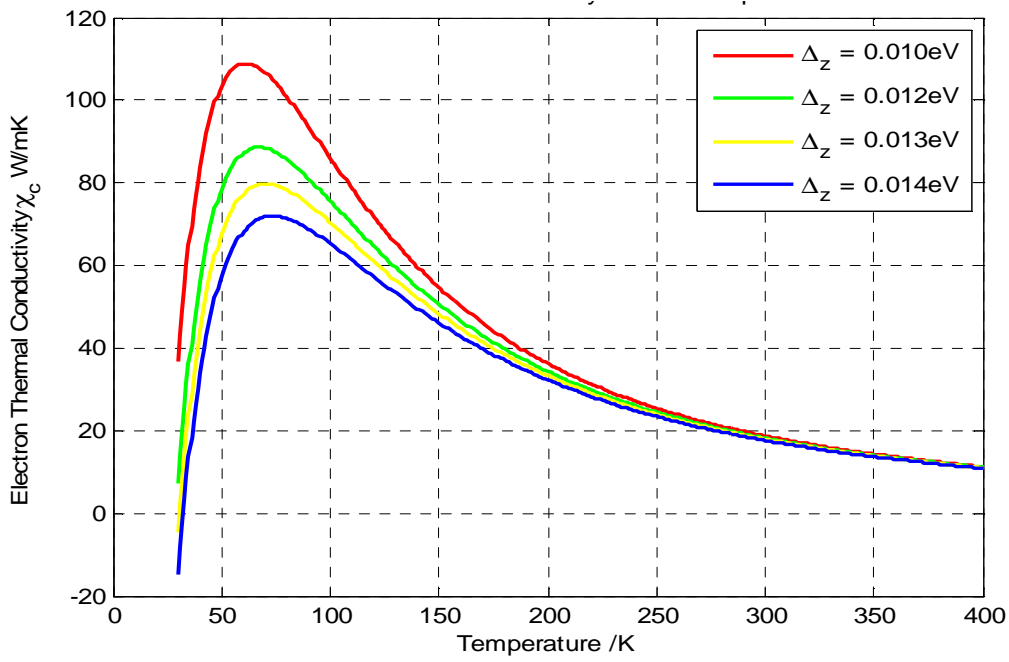
Figure 1a: The dependence of χ_c on temperature T for $\Delta_s = 0.010eV$, $E_s = 1.5 \times 10^7 V/m$ and Δ_z varied from 0.010 to 0.014eV.
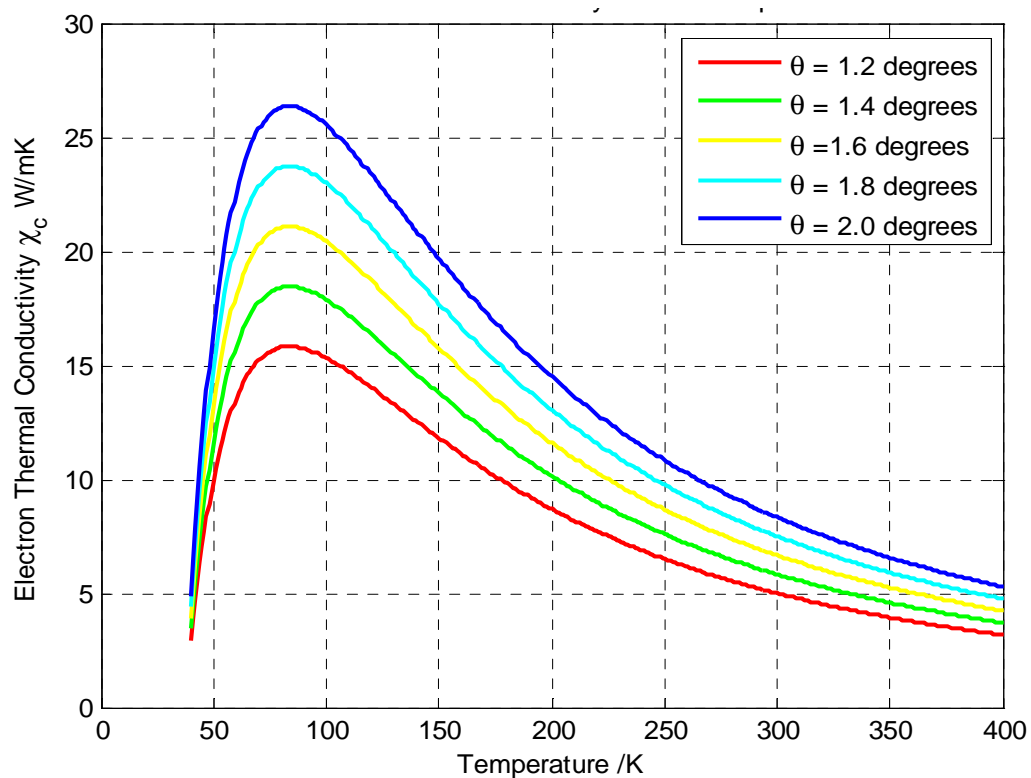
Figure 1b: The dependence of χ_c on temperature T for $\Delta_s = 0.010\text{eV}$, $\Delta_z = 0.017\text{eV}$,. $E_s = 1.5 \times 10^7\text{V/m}$ and GCA θ_h varied from 1.2^o to 2.0^o.
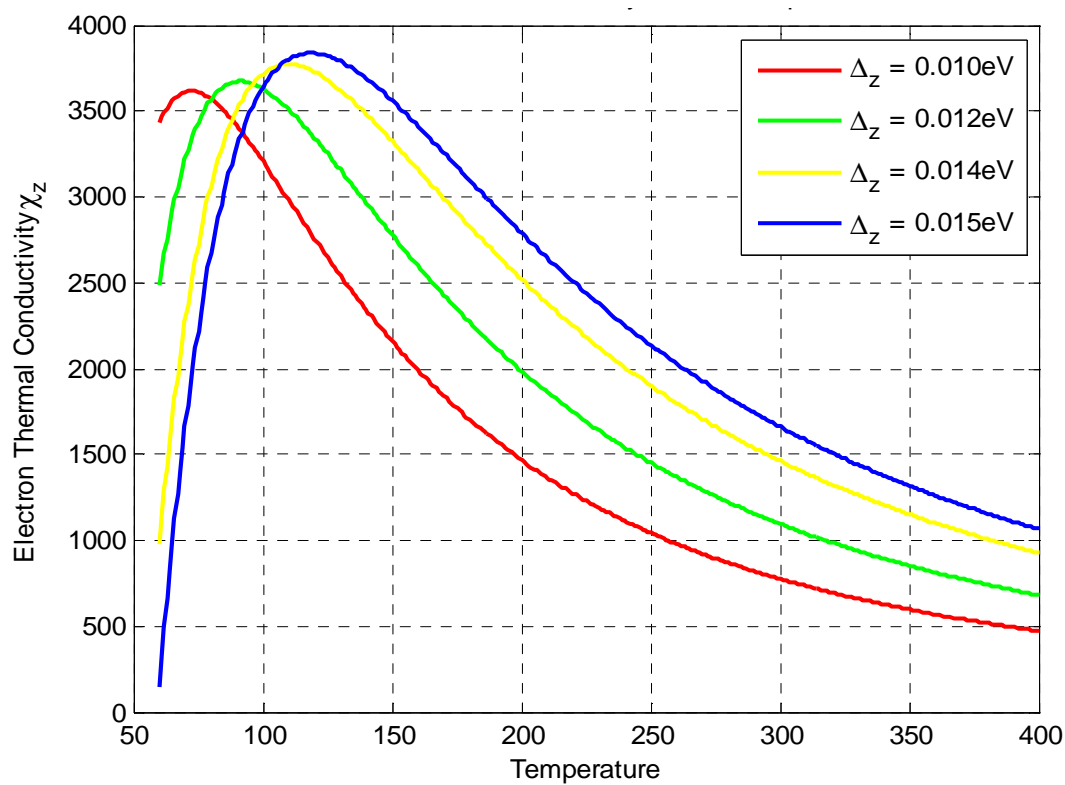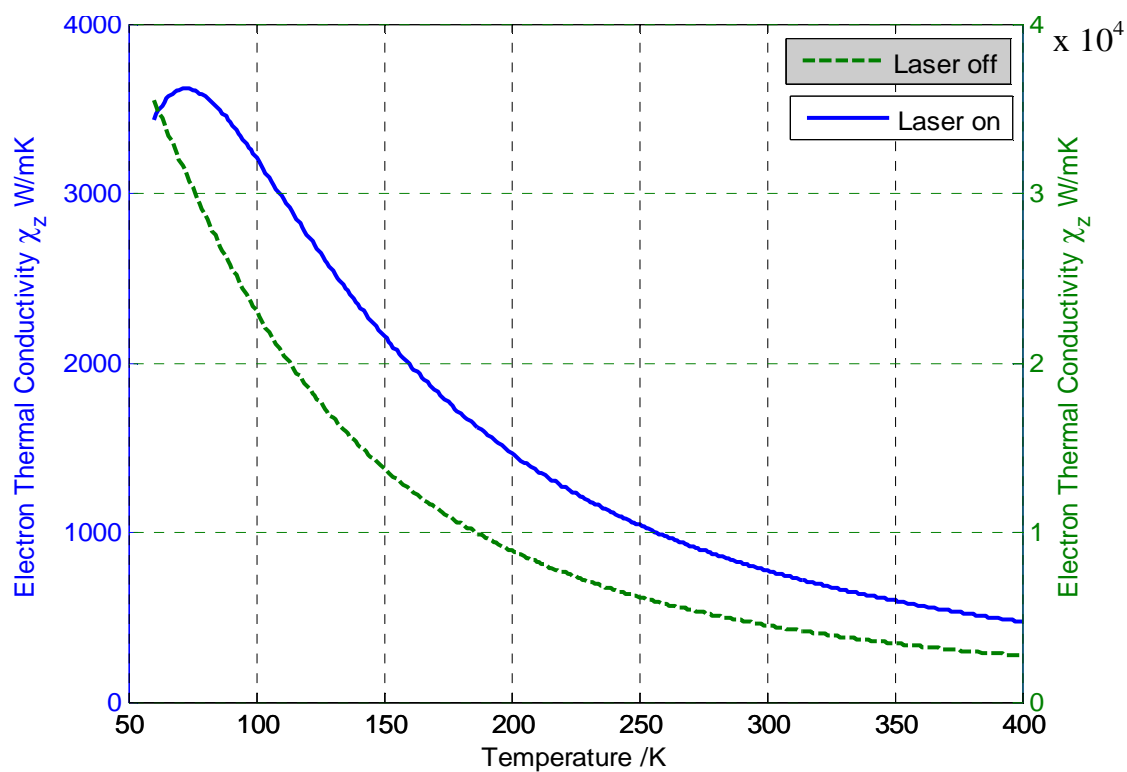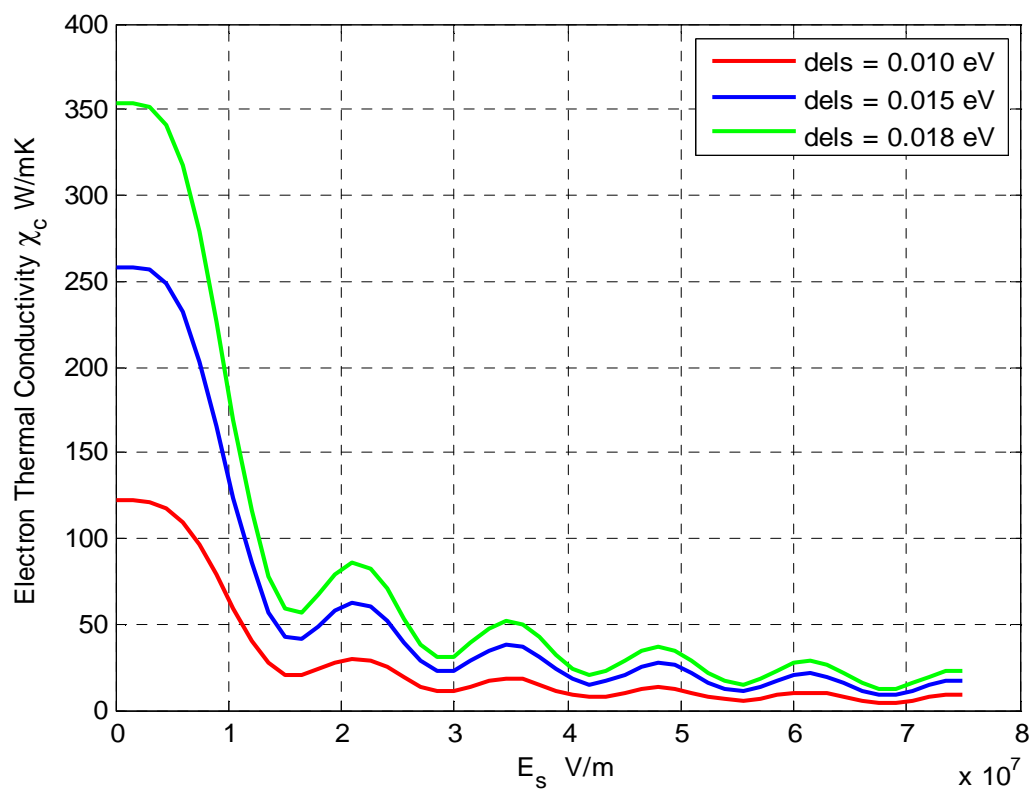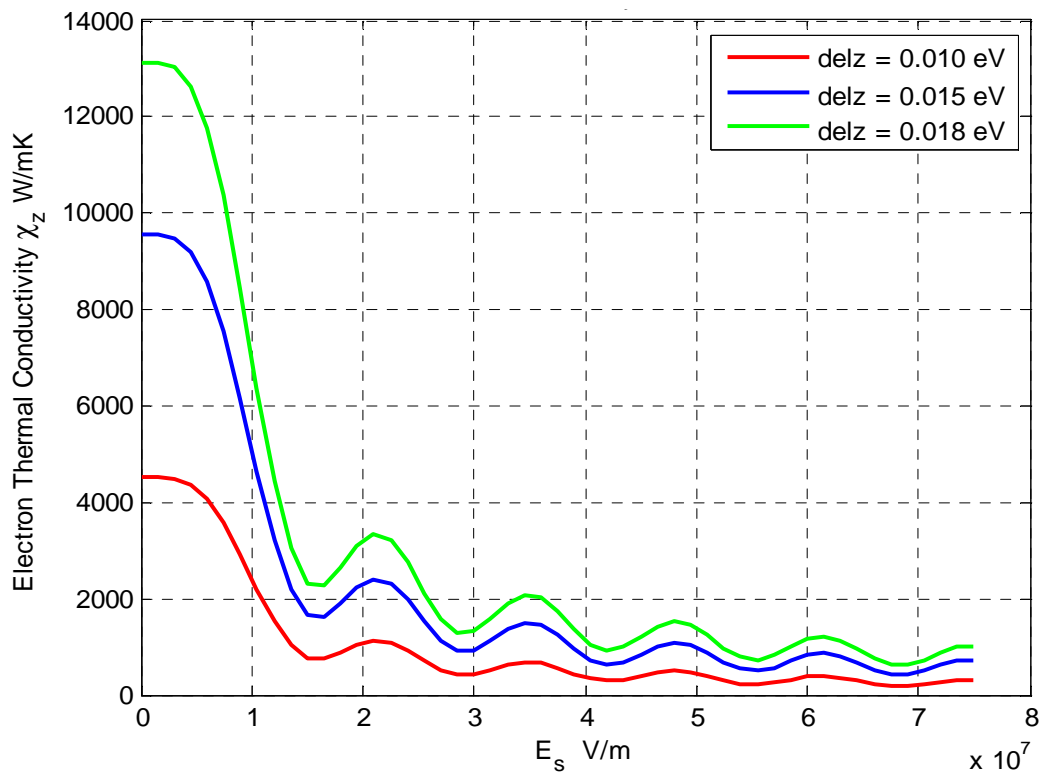
Figure 1c: The dependence of χ_z on temperature T for $\Delta_s = 0.010$eV, $E_s = 1.5 \times 10^7$V/m and Δ_z varied from 0.010 to 0.015eV.
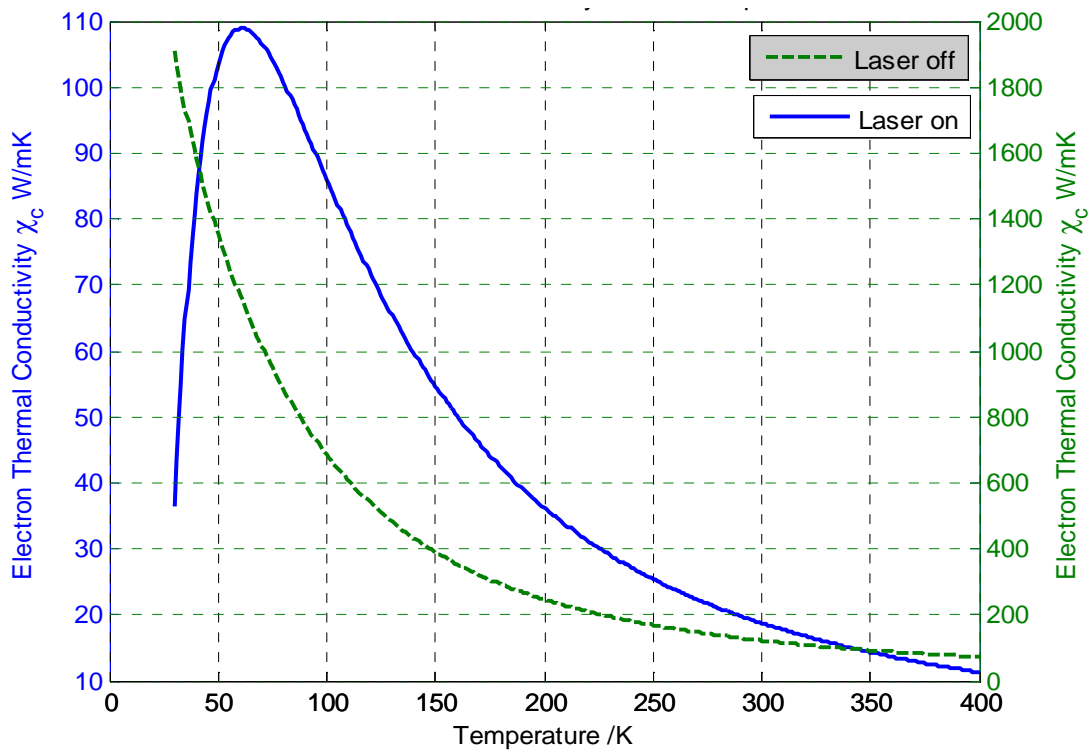
Figure 2a: The dependence of χ_c on temperature T for $\Delta_s = 0.018$eV, $\Delta_z = 0.024$eV, $E_s = 1.5 \times 10^7$V/m and GCA $\theta_h = 4.0^o$ [*Laser off-Right hand side ordinate axis, Laser on- Left hand side ordinate axis*]

Figure 2b: The dependence of χ_z on temperature T for $\Delta_s = 0.018eV$, $\Delta_z = 0.024eV$, $E_s = 1.5 \times 107V/m$ and GCA $\theta_h = 4.0^o$ [*Laser off-Right hand side ordinate axis, Laser on- Left hand side ordinate axis*]

Figure 3a: The dependence of χ_c on E_s at temperature T = 300K for $\Delta_z = 0.010$eV, and Δ_s varied from 0.010 to 0.018eV.

Figure 3b: The dependence of χ_z on E_s at temperature T = 300K for $\Delta_s = 0.010$eV, and Δ_z varied from 0.010 to 0.018eV